Science Advances
AAAS

Supplementary Materials for

Epinephrine promotes breast cancer metastasis through a ubiquitin-specific peptidase 22–mediated lipolysis circuit

Yuanzhang Zhou *et al.*

Corresponding author: Hongjiang Wang, hjwang@dmu.edu.cn; Zhaolin Sun, zlsun56@yeah.net; Deyu Fang, fangd@northwestern.edu

Sci. Adv. **10**, eado1533 (2024)
DOI: 10.1126/sciadv.ado1533

This PDF file includes:

Figure s1

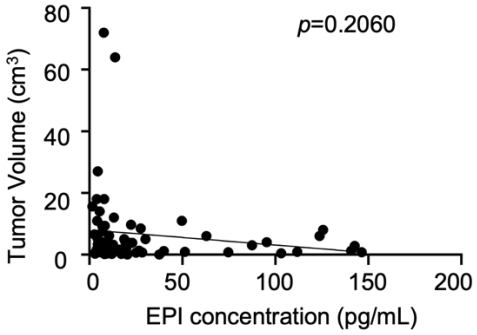

Fig. s1： Statistical analysis to determine the correlation between serum Epi levels and tumor volume. (n = 65). Pearson correlation coefficient was used to as a measure of association.

Figure s2

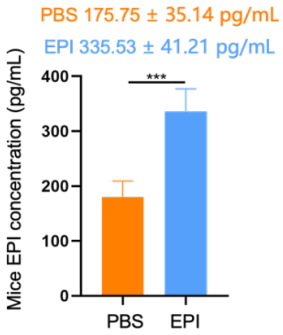

Fig. s2. Analysis of the serum EPI concentrations in mice treated with the EPI and the PBS (N = 10 each group). Data are expressed as mean ± SD. Statistical significance was determined by unpaired Student's *t* test. Statistical significance was concluded at ***$P < 0.001$.

Figure s3

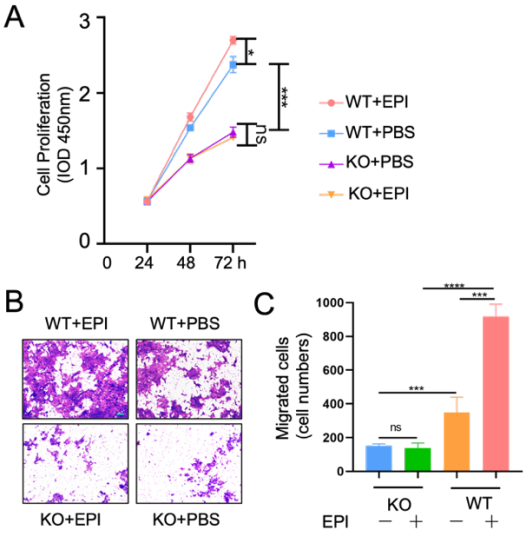

Fig. s3. Analysis of the effects of EPI on 4T1 cell growth and migration. (A) The effect of *USP22* knock out on the 4T1 cell proliferation in the presence of Epi or not were determined by the WST-8

reagent (n = 3). (**B & C**) Transwell assays were conducted to assess the migratory capacity of the indicated types of 4T1 cells (n = 3). Representative images are shown in (B), scar bar: 100μm, and migrated cells were counted from five random fields (C). Statistical significance was determined by unpaired Student's *t* test or one-way ANOVA test. Data are expressed as mean ± SD of three independent experiments. Statistical significance was concluded at $*P < 0.05$, $**P < 0.01$, $***P < 0.001$; ns represents no statistical significance.

Figure s4

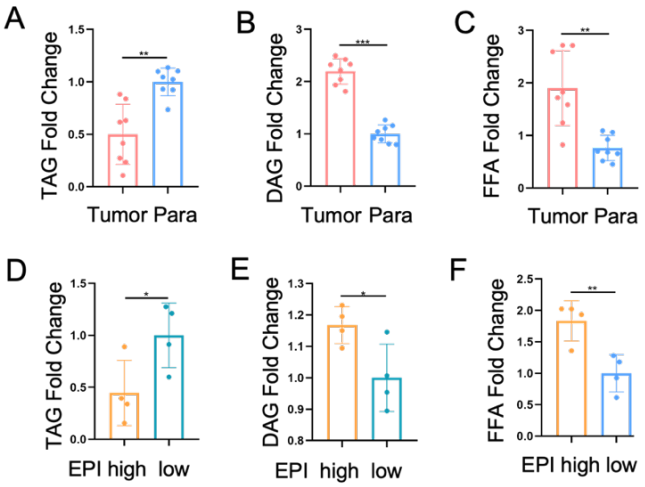

Fig. s4: Analysis of the lipid components in tumor and para-tumor tissues. (**A-C**) Relative levels of TAG (A), DAG (B), FFA (C) in 8 pairs of breast cancer and matched non-tumorous tissues (fold change of mean value of non-tumorous group) (para-tumor, n = 8; tumor, n = 8). (**D-F**) Relative levels of TAG (D), DAG (E), FFA (F) in 8 breast cancer tissues as indicated group (fold change of mean value of Epi ^{low} group) (Epi ^{high}, n = 4; Epi ^{low}, n = 4). Data are expressed as mean ± SD. Statistical significance was determined by unpaired Student's *t* test. Statistical significance was concluded at $*P < 0.05$, $**P < 0.01$. $***P < 0.001$; ns represents no statistical significance.

Figure s5

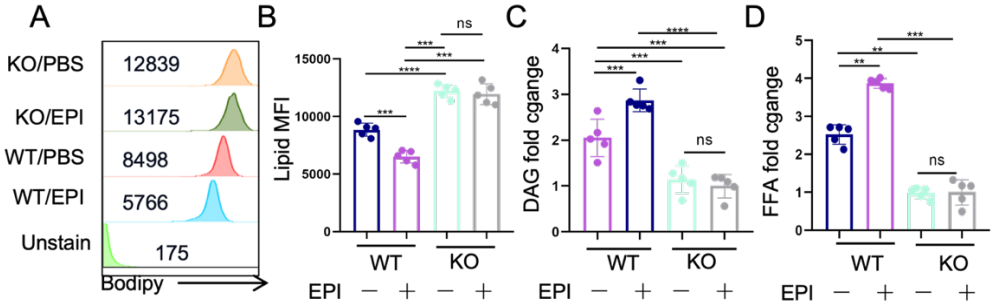

Fig. s5. The effect of EPI on 4T1 cell lipolysis. (A-D) Intracellular lipid analysis in WT and USP22-null 4T-1 cells isolated from the xenograft tumors as shown in Fig. 2Q, including bodipy (A & B), DAG (C) and FFA (D). Data are expressed as mean ± SD of five independent experiments. Statistical significance was determined by one-way ANOVA test or unpaired Student's *t* test. Statistical significance was concluded at $*P < 0.05$, $**P < 0.01$. $***P < 0.001$; ns represents no statistical significance.

Figure s6

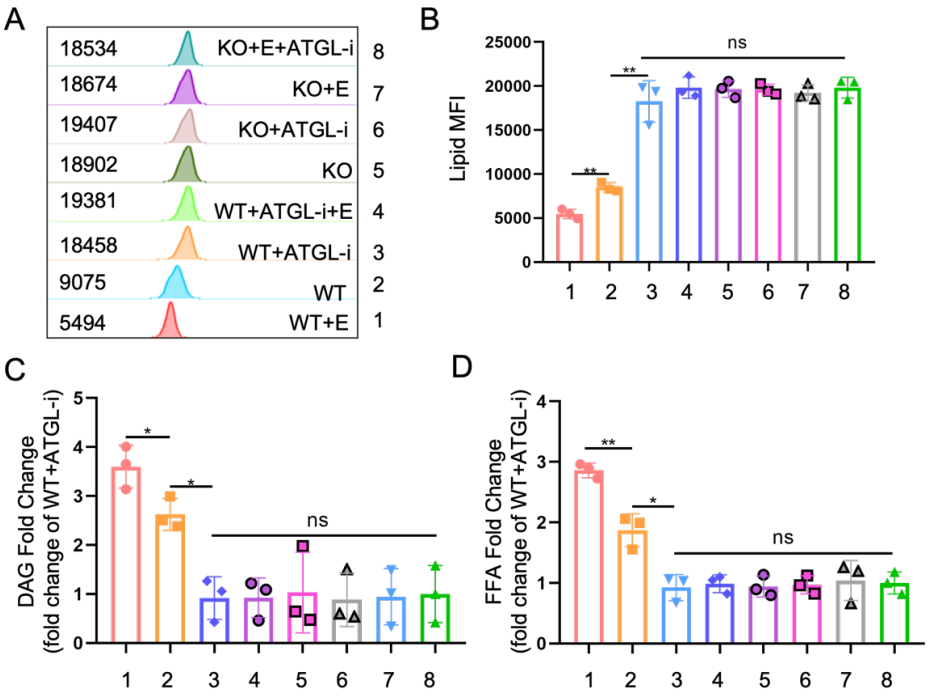

Fig. s6. The effect of ATGL inhibitor on EPI-induced lipolysis. WT and USP22 KO 4T1 cells were treated with EPI or further with ATGL specific inhibitor Atglistatin (50 μM) for 24 hours. **(A & B)** The bodipy staining and **(C & D)** the levels of DAG (C) and FFA (D) were analyzed (N=3). Statistical significance was determined by one-way ANOVA test or unpaired Student's *t* test. Data are expressed as mean±SD of three independent experiments. Statistical significance was concluded at $*P < 0.05$, $**P < 0.01$, $***P < 0.001$; ns: no statistical significance.

Figure s7

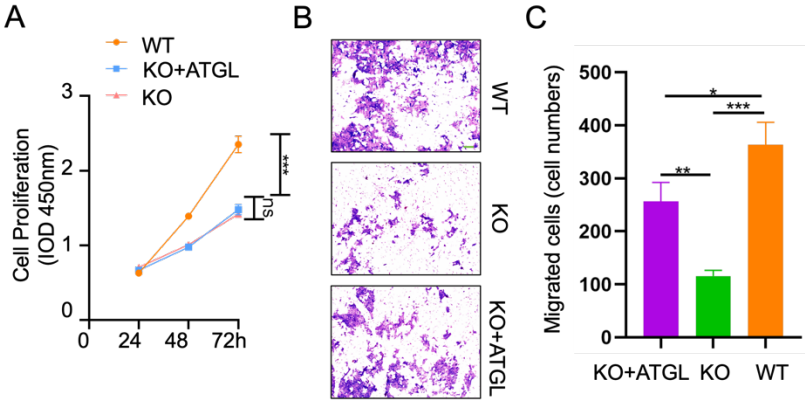

Fig. s7. Analysis of the effects of ATGL expression on USP22-null 4T1 cell growth and migration. **(A)** The effect of overexpression of *ATGL* in the knockout on the 4T1 cell proliferation were determined by the WST-8 reagent. (**B-C**) Transwell assays were performed to evaluate the migratory capacity of the indicated types of 4T1 cells (n = 3). Representative images are presented in (B), scar bar: 100μm, and the number of migrated cells was quantified from five random fields (C). Statistical significance was determined by unpaired Student's *t* test or one-way ANOVA test. Data are expressed as mean ± SD of three independent experiments. Statistical significance was concluded at $*P < 0.05$,

**$P < 0.01$, ***$P < 0.001$; ns: no statistical significance.

Figure s8

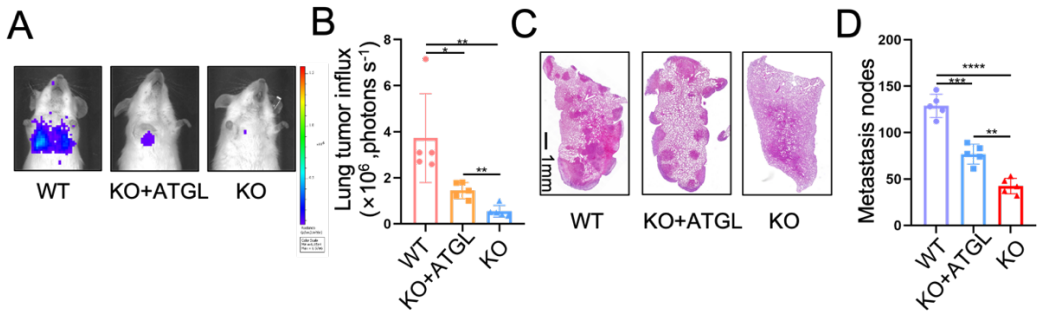

Fig. s8: Analysis of the effects of ATGL expression on USP22-null 4T1 tumor metastasis. (A-D) A total of 0.5*10^5 WT, USP22-KO + ATGL 4T1 cells or USP22-KO 4T1 cells transduced with ATGL were injected via the tail vein into BALB/C mice. Lung metastases were measured by luminol fluorescence (A & B) and H & E staining (C & D). Statistical significance was determined by unpaired Student's *t* test or one-way ANOVA test. Data are expressed as mean ± SD of five independent experiments. Statistical significance was concluded at *$P < 0.05$, **$P < 0.01$, ***$P < 0.001$; ns: no statistical significance.

Figure s9

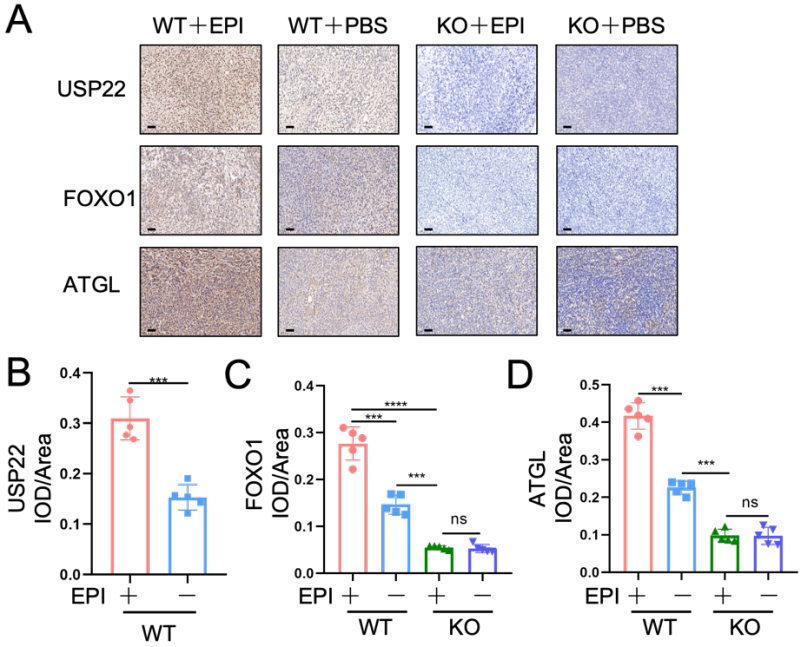

Fig. s9. Analysis of USP22, FOXO1 and ATGL expression levels by immunohistochemistry in syngeneic tumor tissues as shown in Fig. 2Q. Representative images **(A),** scale bar: 50 μm and quantification data **(B-D)** are shown. Statistical significance was determined by one-way ANOVA test or unpaired Student's *t* test. Data are expressed as mean ± SD of five independent experiments. Statistical significance was concluded at *$P < 0.05$, **$P < 0.01$, ***$P < 0.001$; ns: no statistical significance.

Figure s10

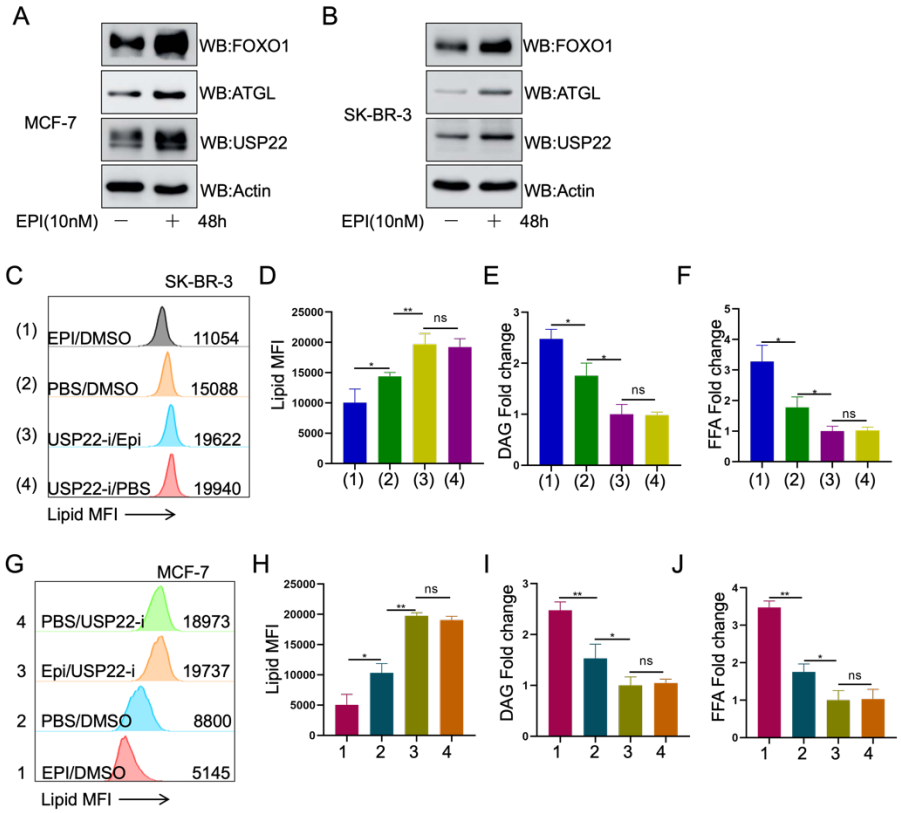

Fig. 10. Analysis of EPI-induced USP22 and lipolysis in MCF-7 and SK-BR-3 cells. (A & B) Analysis of USP22, ATGL, FOXO1 protein expression in MCF-7 cells (A) and SK-BR-3 cells (B) after treated with Epi for 48h. **(C-J)** Intracellular lipid analysis, including bodipy, DAG and FFA in indicated types of SK-BR-3 cells (C-F) or MCF-7 cells (G-J). (n = 3). Statistical significance was determined by one-way ANOVA test or unpaired Student's *t* test. Data are expressed as mean ± SD of three independent experiments. Statistical significance was concluded at $*P < 0.05$, $**P < 0.01$, $***P < 0.001$; ns: no statistical significance.

Figure s11

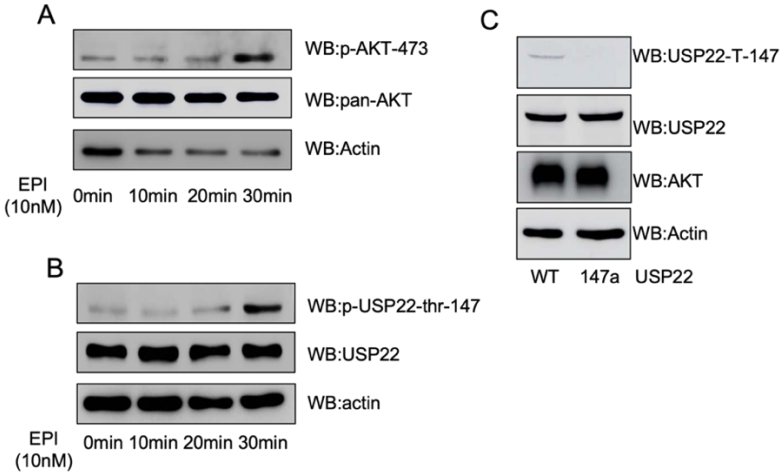

Fig. s11. Analysis of EPI-induced AKT phosphorylation. (A) Immunoblot analysis of p-AKT-473 protein expression in MDA-MB-231 cells treated with EPI or PBS for indicated times. **(B).**

Immunoblot analysis of p-USP22-thr-147 protein expression in MDA-MB-231 cells treated with EPI or PBS for indicated times. **(C)** WT or USP22/T147A mutants with or without AKT were transfected to USP22 KO 4T1 cells. USP22 phosphorylation was determined by immunoblotting with anti-p-147-USP22 Ab (top panel). The expression levels of total USP22 (middle panel) and AKT (bottom panel) were confirmed.

Figure s12

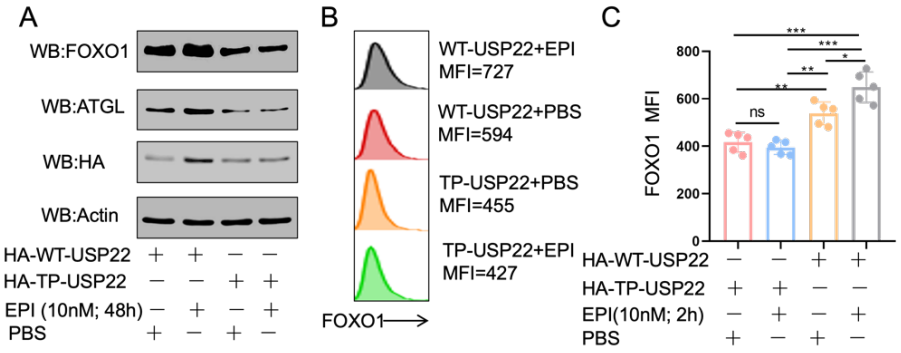

Fig. s12. The effect of USP22 phosphorylation on lipolysis in 4T1 cells. (A) Analysis of USP22, FOXO1, ATGL protein expression in USP22-KO MDA-MB-231 cells transfected with the WT-USP22 plasmid or the TP-USP22 plasmid and treated with Epi or PBS**. (B-C)** The effect of EPI on FOXO1 protein expression in USP22-KO MDA-MB-231 cells transfected with the WT-USP22 plasmid or the TP-USP22 plasmid. Statistical significance was determined by one-way ANOVA test or unpaired Student's *t* test. Data are expressed as mean ± SD of five independent experiments. Statistical significance was concluded at $*P < 0.05$, $**P < 0.01$, $***P < 0.001$; ns: no statistical significance.

Figure s13

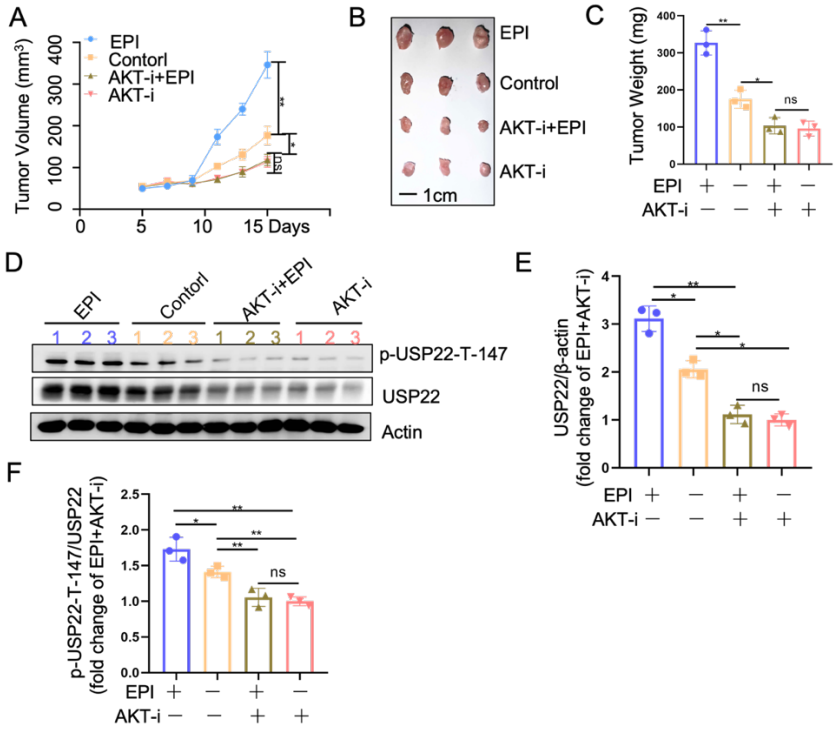

Fig. s13. The effect of AKT inhibition on USP22 phosphorylation in tumors. (A-C) Triple-negative

breast cancer 4T1 cells were injected into mammary fat pad of BALB/c mice (N=3 each group). Tumor volume (A), and tumor weight (B & C) were measured. (D) Analysis of USP22 and p-USP22-T-147 protein expression in tumor tissue from (B). (**E-F**) Quantitative analysis of USP22 and p-USP22-T-147 protein expression in the (D). Beta-actin used as a control to quantify the expression of USP22 (E). Quantification of phosphorylation is presented as ratios of signal intensities of phosphorylated protein (p-USP22-T-147) to total protein (USP22) (F). Statistical significance was determined by one-way ANOVA test or unpaired Student's *t* test. Data are expressed as mean ± SD of three independent experiments. Statistical significance was concluded at $*P < 0.05$, $**P < 0.01$, $***P < 0.001$; ns: no statistical significance.

Figure s14

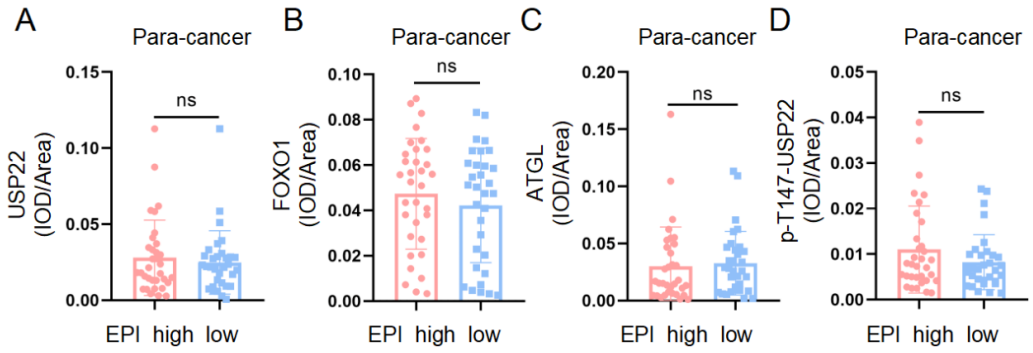

Fig. s14: (A) Analysis of USP22(A), FOXO1(B), ATGL(C), p-USP22-T147(D) expression of human para-breast cancer tissues in EPI ^{high} and EPI ^{low} patients (Epi^{low}, n = 33; and Epi^{high}, n = 32). Statistical significance was determined by unpaired Student's *t* test. Data are expressed as mean ± SD. Statistical significance was concluded at $*P < 0.05$, $**P < 0.01$, $***P < 0.001$; ns: no statistical significance.

Figure s15

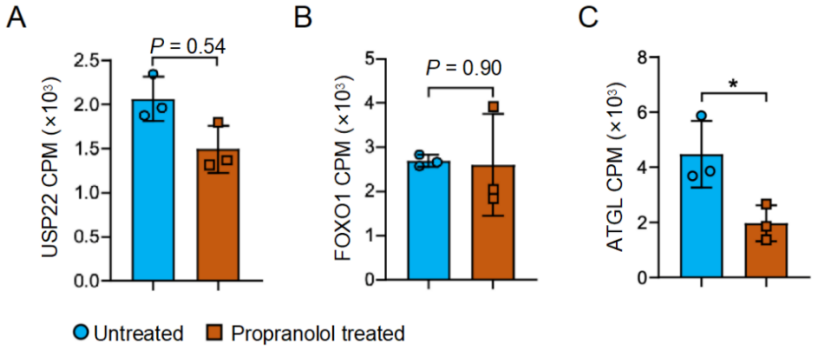

Fig. s15: Analysis of Usp22 **(A),** Foxo1 **(B)** and Atgl **(C)** expressions of GSM5740291. The data set was from three repeated RNA-seq analysis of the human medulloblastoma ONS-76 cells treated with propranolol or control PBS. CPM: counts per million cells. Unpaired Students *t* test was used for statistical analysis, * $p < 0.05$.

Figure s16.

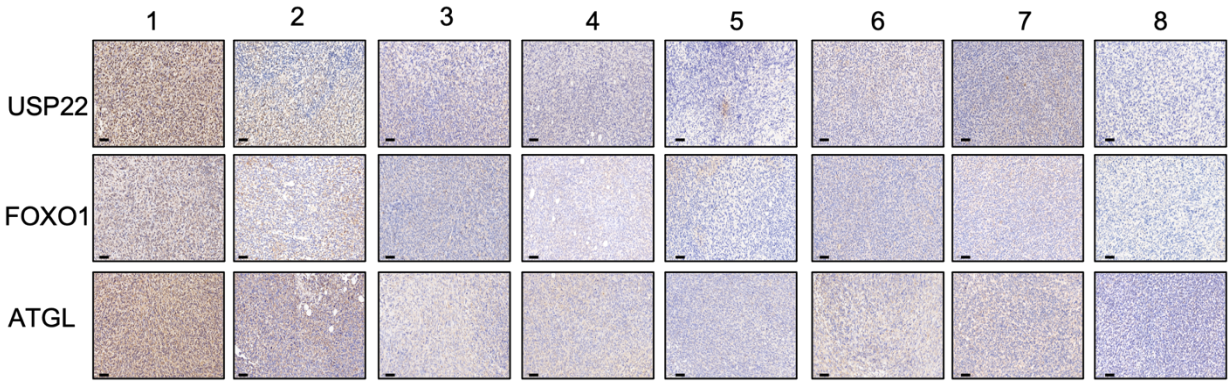

Fig. s16: Representative immunohistochemistry photomicrographs of tissues stained with USP22, FOXO1, ATGL from the tumor in the Fig. 7A, scale bar: 50 μm.

Supplementary Table1 Association of plasma epinephrine level with clinical and pathological characteristics of breast cancer patients

Variable	All case N (%)	Patient # Plasma EPI Low & High		P[A]
		Low	High	
HER2				0.321
−	52 (80)	28	24	
+	13 (20)	5	8	
PR				0.812
−	15 (23)	8	7	
+	50 (77)	25	25	
ER				0.294
−	11 (16.9)	4	7	
+	54 (83.1)	29	25	
Tumor Stage				0.426
0	1 (1.55)	0	1	
1	27 (41.5)	13	14	
2	31 (47.7)	16	15	
3	5 (7.7)	4	1	
4	1 (1.55)	0	1	

[A] χ^2test; n = 65. ER+：ER ≥+ and ≥1% ； ER-：ER＜1%； PR+：PR≥+and≥1%； PR-：PR＜1%; HER2+：HER2 3+ or HER2 2+ and FISH +； HER2-：HER2 0 or 1+ or HER2 2+.

Supplementary Table 2. gRNAs used forUSP22 KO in mouse and human breast cancer cells.

Sample	sg-RNA Sequence
sgRNA for human USP22	sgRNA-A1： TTCAAAGCAGCCAATACTCCAGG sgRNA-A2: GATGCGAGCCCTTCGTGTTGAGG
sgRNA for mouse USP22	sgRNA-A1: GTTGTCCGCATTAACAATGCTGG sgRNA-A2: AGATGTGGACGGTGCACGCGAGG

Supplementary Table 3: PCR primers for USP22 analysis.

Primer for PCR	Sequence
Primer for exon of human USP22	For: 5’- CCCCTGTACTTAAGGTAAGAGTAGC -3’ Rev: 5’- TAGCATGCACTGAGGTTGGG -3’
Primer for exon of mouse USP22	For: 5’-ATTCCTTCATTCCCAGGGCG-3’ Rev: 5’-CAGGGATCATGTCGGGAAGT-3’

Supplementary Table 4: Primers used for ChIP-qPCR analysis.

Primer for ChIP	sg-RNA Sequence
Primer for promoter of PNPLA2	For 5′- TTCATGGGTGAGGGTGCTTC− 3′ Rev: 5′- ACATCACTCCCTCATGGCAG − 3

Supplementary Table 5. Abs used for the study.

Antibodies reagent	Source	Catalog
FOXO1	Cell Signaling Technology	2880
USP22	Abcam	ab195289
pan-AKT	Proteintech	60203-2-Ig
p-AKT-473	Cell Signaling Technology	4051
Phospho-USP22(thr147)	Invitrogen	PA5-105351
Phosphoserine/threonine	Invitrogen	MA5-38234
ATGL	Absin	abs137233
HA-tag	Cell Signaling Technology	3724S
His-tag	Cell Signaling Technology	12698S
Flag-HRP	Sigma	A8592
Flag	Sigma	F-1804
HA-tag	Santa-cruze	sc-7392
myc-tag	Cell Signaling Technology	2276S
myc-HRP	Cell Signaling Technology	2040S
β-actin	Proteintech	66009-1-lg
GAPDH	Proteintech	10494-1-AP
anti-rabbit IgG antibody	Cell Signaling Technology	7074S
anti-mouse IgG antibody	Cell Signaling Technology	7076S

Supplementary Table 6. Primers for real-time RT-PCR analysis.

Primer name (RT-qPCR)	Sequence(5'-3')
human-ATGL-F	CCATCACAGTGTCCCCCTTC
human -ATGL-R	AACTGGATGCTGGTGTTGGT
human -USP22-F	CTGGGACATCAGCTTGGATCT
human -USP22-R	CTTTCCCCGTTTACCACGTTG
human -FOXO1-F	TTCACCCAGCCCAAACTACC
human -FOXO1-R	GAGTCCAGGCGCACAGTTAT
human -ACTB-F	GGGAAATCGTGCGTGACATT
human -ACTB-R	GGAACCGCTCATTGCCAAT